CRISPR-Cas is beneficial in plasmid competition, but limited by competitor toxin-antitoxin activity when horizontally transferred.

David Sünderhauf*[1], Jahn R. Ringger[1+], Leighton J. Payne[2], Rafael Pinilla-Redondo[2], William H. Gaze[3], Sam P Brown[4, 5], Stineke van Houte*[1]

*corresponding authors; DS: david@sunderhauf.net, SvH: C.van-Houte@exeter.ac.uk

[1] Environment and Sustainability Institute, University of Exeter Penryn Campus, Penryn, TR10 9FE, UK

[2] Section of Microbiology, Department of Biology, University of Copenhagen, Copenhagen, Denmark

[3] European Centre for Environment and Human Health, University of Exeter Penryn Campus, Penryn, TR10 9FE

[4] School of Biological Sciences, Georgia Institute of Technology, Atlanta, Georgia, USA

[5] Center for Microbial Dynamics and Infection, Georgia Institute of Technology, Atlanta, Georgia, USA

[+]current address: Department of Environmental Sciences, University of Basel, 4051 Basel, Switzerland

ORCIDs:

DS - 0000-0002-8007-3351; JRR - 0009-0002-1831-3630; LJP - 0000-0003-2305-6827; RPR - 0000-0003-3521-460X; WHG - 0000-0002-9345-6204; SPB - 0000-0003-1892-9275; SVH - 0000-0001-7047-1308

Abstract

Bacteria can encode dozens of different immune systems that protect them from infection by mobile genetic elements (MGEs). MGEs themselves may also carry immune systems, such as CRISPR-Cas, to target competitor MGEs. It is unclear when this is favoured by natural selection, and whether toxin-antitoxin (TA) systems — common competitive mechanisms carried by plasmids — can alter their efficacy. Here, we develop and test novel theory to analyse the outcome of competition between plasmids when one carries a CRISPR-Cas system that targets the other plasmid. Our model and experiments reveal that plasmid-borne CRISPR-Cas is beneficial to the plasmid carrying it when the plasmid has not recently transferred to a new host. However, CRISPR-Cas is selected against when the plasmid carrying it transfers horizontally, if a resident competitor plasmid encodes a TA system that elicits post-segregational killing. Consistent with a TA barrier to plasmid-borne CRISPR-Cas, a bioinformatic analysis reveals that naturally occurring CRISPR-Cas-bearing plasmids avoid targeting other plasmids with TA systems.

Our work shows how the benefit of plasmid-borne CRISPR-Cas is severely reduced against TA-encoding competitor plasmids, but only when plasmid-borne CRISPR-Cas is horizontally transferred. These findings have key implications for the distribution of prokaryotic defences and our understanding of their role in competition between MGEs, and the utility of CRISPR-Cas as a tool to remove plasmids from pathogenic bacteria.

Introduction

Mobile genetic elements (MGEs) are widely distributed throughout the prokaryotic tree of life and shape the ecology and evolution of bacterial populations. Conjugative plasmids are the MGEs most proficient at horizontally transferring genes (including antimicrobial resistance genes) through bacterial communities [1], and frequently co-infect the same bacterial cell [2]. Prokaryotic immune systems are abundant in prokaryotic genomes and can alter not only how the bacterial host interacts with MGEs, but also how co-infecting MGEs interact with each other [3,4]. However, the unique selection pressures faced by immune systems that are encoded on MGEs have not been investigated.

CRISPR-Cas is an adaptive immune response whereby a ribonucleoprotein complex acts as an RNA-guided DNA or RNA nuclease and specifically recognises and cleaves an invading MGE (and/or its transcripts), based on a short sequence stored in the CRISPR locus as a “spacer” during a previous infection (reviewed in [5]). CRISPR-Cas systems are found on ~3% of plasmids [6], where they play a role in competition between plasmids (reviewed in [7]): plasmids’ CRISPR spacers tend to match other, competing plasmids [6,8].

In response, plasmids may invest in traits that give them a fitness advantage. These can be either through direct interference with CRISPR-Cas, such as anti-CRISPRs [9], or through CRISPR-Cas-independent features such as plasmid incompatibility [10], Bet/Exo systems [11], entry exclusion [12], and toxin-antitoxin (TA) systems [13]. Of these, TA systems are highly prevalent and carried by ~35% of plasmids [14]. TA systems function by simultaneous production of a toxin and a short-lived antitoxin. If the plasmid — and therefore the TA genes it carries — are removed, the

toxin will be freed up to harm or kill the bacterial host. This addictive nature of TA systems means their removal is strongly selected against [13] (including removal by chromosomally-encoded CRISPR-Cas [15,16]), and this phenomenon is theorised to be beneficial to plasmid competition [17–19]. In line with this, TA systems were identified as a barrier to plasmid removal when using CRISPR-Cas or incompatibility-based technologies [20,21].

Both TA systems and CRISPR-Cas immune systems are important during within-cell plasmid competition [8,19], but it is unclear how selection acts on these traits when they directly compete with one another. To test this, we constructed a mathematical model to predict the outcome of plasmid competition between a CRISPR-Cas-bearing and a TA-bearing plasmid within an individual host, dependent on whether the CRISPR-Cas plasmid was acting offensively (i.e., invaded a new host) or defensively (i.e., protected its host from competitor invasion). We tested model predictions using an experimental system where a CRISPR-Cas-bearing and a TA-bearing IncP plasmid competed for *E. coli* hosts in similar ecological scenarios. Finally, we further tested our theory and generalized our experimental results by bioinformatically analysing TA carriage of target plasmids of naturally occurring plasmid-borne CRISPR-Cas systems. Together, our theory, experiments, and bioinformatics analyses show that when CRISPR-Cas-bearing plasmids are acting offensively and invading a new host, the otherwise universal benefit of CRISPR-Cas to plasmid competition is limited by TA carried on competitor plasmids. This work highlights the limitations of CRISPR-Cas in plasmid competition and underlines the advantages of TA systems to plasmid spread and persistence.

Results

Mathematical modelling predicts that the benefit of CRISPR-Cas depends on toxin-antitoxin (TA) activity of competitor plasmids.

Both CRISPR-Cas and TA systems are implicated in plasmid-level competition [8,19]. In a mathematical analysis, we set out to formalise the relative benefits of CRISPR-Cas to a plasmid when competing with a plasmid encoding TA, depending on asymmetries due to distinct offensive versus defensive roles of CRISPR-Cas and TA. A defensive role refers to a plasmid remaining resident in a cell line. In contrast, an offensive role refers to horizontal transfer of a plasmid to a new host and becoming a newly arrived invader in a cell.

To formalise plasmid competition dynamics, we begin with a simple conceptualisation of plasmid competition (Figure 1A). Our approach focuses on cells co-infected with both plasmids (*CT* and *TC* cells), with plasmids differentiated by their order of arrival. *C* represents cells where a CRISPR-Cas plasmid is resident, while *T* represents cells where a TA plasmid is resident. In the event *C* cells are infected by a TA-plasmid, we have a *CT* cell containing both a resident CRISPR-Cas plasmid and an invading TA plasmid. Conversely, *TC* cells are created when a *T* cell acquires a CRISPR-Cas plasmid.

Our model defines transition rates from co-infected states (*CT* or *TC*) to singly infected states (*C* or *T*) (arrows in Figure 1AB). These transition rates are defined by plasmid segregational loss (baseline rate s), modified by *C*- and *T*-specific traits of CRISPR-Cas-induced enhanced segregation x (blue in Figure 1A; $x > 1$ implies multiplicatively increased segregation rate $x \cdot s$) and TA-induced probability of post-segregational killing (PSK) y (red in Figure 1A). Asymmetries in parameter values

between resident and invader roles are captured by subscripts *r* and *i*. In the event of PSK, liberated resources (nutrients, space) can enhance the growth of remaining *C* or *T* cells, weighted by parameter *f* [19] where f_r refers to the benefit given to cells containing the previously resident plasmid (*T* for *TC* cells and vice versa). Given lower plasmid copy number and lower gene expression for invading versus resident plasmids [22], our default assumptions are $s_i > s_r$; $x_r > x_i \geq 1$; $1 > y_r > y_i \geq 0$. Given spatial structuring so that *T* cells are enriched in the neighbourhood of *TC* cells (and vice versa for *C* near *CT* cells), we further assume $1 > f_r + f_i > f_r > f_i \geq 0$. The resulting transition rates (Figure 1AB, equations E1-E4) are used to define CRISPR-Cas competition summary metrics Δ_C, which capture whether CRISPR-Cas investment *x* results in more transitions to *C* than to *T* cells ($\Delta_C > 0$), or vice versa ($\Delta_C < 0$). These metrics are calculated for both the context when the CRISPR-Cas plasmid is resident (Figure 1AC, equation E5), and when it is an invader (Figure 1BD, equation E7).

Analysis of Δ_C of CRISPR-Cas plasmids provided the following core predictions concerning the impact of CRISPR-Cas and TA investments (*x* and *y*) on their relative competitive success (derivations in Supplementary Results 1): Firstly, in the absence of PSK (no TA; $y = 0$), increasing investment in CRISPR-Cas *x* always increases CRISPR-Cas competitive success, regardless of whether in a defensive (Figure 1C) or offensive role (Figure 1D). Secondly, in the presence of PSK ($y > 0$), increasing CRISPR-Cas investments is still beneficial in a resident context (Figure 1C), but can become detrimental in an offensive role, given sufficiently strong resident TA y_r (Figure 1D, area above the dashed line). Analytical conditions for this qualitative shift in response are defined in Supplementary Results 1.

In conclusion, our model predicted an asymmetric outcome of plasmid competition, depending on CRISPR-Cas mode of action. When resident, investing in stronger CRISPR-Cas always benefitted its own plasmid. In offense CRISPR-Cas switched from an asset to a liability in plasmid competition, dependent on a sufficiently strong TA response on the competitor plasmid.

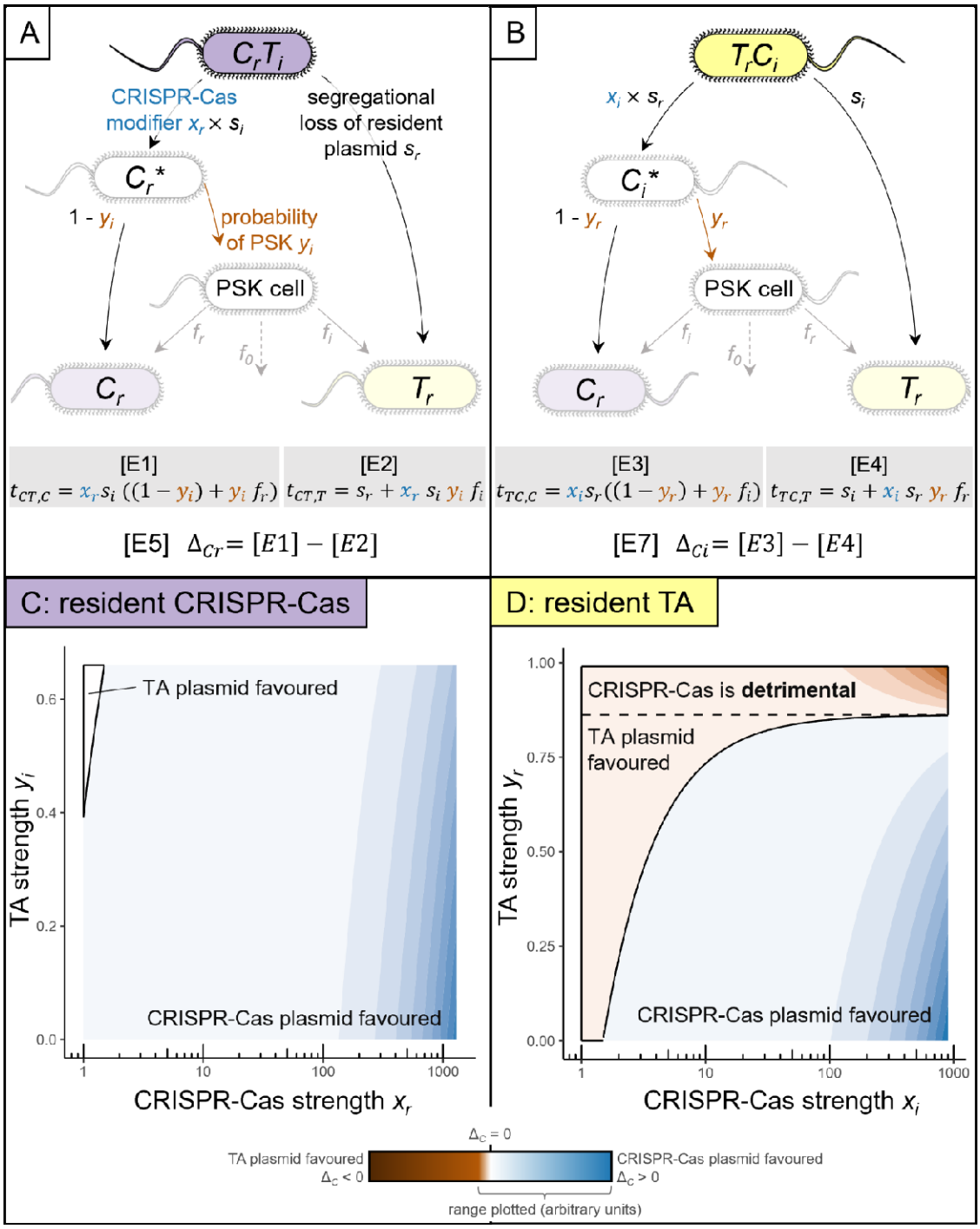

Figure 1: Mathematical modelling predicts that CRISPR-Cas has a greater potential to benefit its plasmid in defence than in offense.

A-B: Structure of the mathematical model when a CRISPR-Cas plasmid is the resident (A) or the invader plasmid (B). We consider seven distinct cell types: *C*

(CRISPR-Cas bearing) and *T* (TA-bearing) plasmids reside in host cells; *CT* denotes a *C* cell that has been invaded by a *T* plasmid and vice versa; C_r* and C_i* cells have undergone segregational loss of a *T* plasmid, and the fate of PSK is not yet resolved; PSK cells are dead cells after post-segregational killing. When the plasmids co-reside, they are subject to basic biological parameter *s* (segregational loss). CRISPR-Cas and TA alter parameter *s* by their own modes of action *x* and *y* respectively. Parameter *f* describes the positive effect PSK cells have on growth of nearby cells, where f_r describes the benefit to cells containing the previously resident plasmid. All parameters adopt distinct values when their respective plasmids are resident (*r*) or invasive (*i*).

C-D: Plasmid competition summary metric of the *C* plasmid, in either resident (Δ_{Cr}) or invader role (Δ_{Ci}). Values >1 describe plasmid competition resolved in favour of the CRISPR-Cas plasmid, and values <1 describe plasmid competition resolved in favour of the TA plasmid (highlighted area) as a function of strength of CRISPR-Cas system *x* and strength of TA system *y*.. Both *x* and *y* adopt different maximum values depending on which plasmid is resident (maximum y_i = 0.66; maximum y_r = 0.99; maximum x_r = 1300; maximum x_i = 900). Parameter choices are specified in Supplementary Results 1.

<u>Experimentally competing a CRISPR-Cas and TA plasmid showed a universal CRISPR-Cas benefit in defence, but not in offense.</u>

Our mathematical modelling predicts that the benefits of a plasmid-borne CRISPR-Cas system are limited during competition with TA plasmids. We sought to test these

predictions experimentally in a model system where we could modulate CRISPR-Cas and TA strength in a binary way. To this end, we used competitor plasmids pKJK5::csg (IncP1ε) and RP4 (IncP1α) in *Escherichia coli* hosts as models to examine how selection acts on plasmid-encoded CRISPR-Cas under defensive and offensive modes of action (Figure 2AB). Due to plasmid incompatibility resulting in segregational loss, these plasmids cannot be co-maintained in the same host indefinitely but can co-exist for several generations [23], giving an ample window of opportunity for plasmid competition within the same bacterial host. Plasmid pKJK5::csg was engineered to carry a minimal Type II CRISPR-Cas9 system [24], and we turned CRISPR-Cas activity on or off by using two isogenic plasmid variants that only differed in their respective fixed targeting specificity (Figure 2A, see Methods). Competitor plasmid RP4 naturally carries the Type II TA system *parABCDE*, where *parABC* form a segregational stability system and *parDE* code for a TA system that inhibits DNA gyrase, leading to cell filamentation and cell death of plasmid-free segregants [25–27]. We turned RP4's TA activity off by supplying an expression vector engineered to carry RP4's *par* TA operon (pCDF1b_par) to all potential plasmid hosts, thus allowing supply of the antitoxin *in trans* and negating the PSK effect of RP4's TA system. As a control, empty vector pCDF1b was supplied in all treatments where TA remained turned on (Figure 2A). These vectors were maintained throughout all experiments in the absence of antibiotic selection (Figure S1).

To assess plasmid competition outcome under different modes of CRISPR-Cas action, we set up mating assays including three differentially tagged *Escherichia coli* DH5α hosts with different plasmid content (Figure 2B). In this way, we could track plasmid competition when CRISPR-Cas was acting defensively (a pKJK5 host was

invaded by RP4) and when CRISPR-Cas was acting offensively (an RP4 host was invaded by pKJK5). Further, we included an intermediate scenario where both plasmids invade an initially naïve, plasmid-free host, so that the mode of action of CRISPR-Cas could be either offensive or defensive. After solid-surface filter mating, we calculated the outcome of plasmid competition by measuring the relative abundance of each plasmid in each host by selective plating (competitive ratio; the log odds ratio of the proportion of pKJK5 over RP4 carriage within hosts; positive values indicate that CRISPR-Cas plasmid pKJK5 was more abundant in its host, and negative values indicate that TA plasmid RP4 was more abundant).

A low limit of detection of TA plasmid RP4 in the defensive CRISPR-Cas host (Figure 2C) led to missing datapoints, especially where TA was turned off, and did not allow us to draw quantitative conclusions of the impact of TA status on the benefit conveyed by CRISPR-Cas in this host. Nonetheless, this analysis revealed that when CRISPR-Cas was acting defensively, the CRISPR-Cas plasmid pKJK5 won the competition in every case where CRISPR-Cas was switched on (Figure 2C; competitive ratio = 1.41 (N=1) and 1.94 ± 0.0085 respectively; significantly higher than 0 with $p < 0.001$ after T-test and Bonferroni adjustment for multiple testing with $\alpha = 0.005$). In stark contrast, when CRISPR-Cas was acting offensively, switching on CRISPR-Cas had a differential effect depending on TA status of the competitor plasmid. When TA was absent from the competitor, switching on CRISPR-Cas brought little or no benefit to pKJK5 (Figure 2D; competitive ratio = 0.32 ± 0.13; $p = 0.07$). However, when the competitor plasmid's TA was switched on, switching on CRISPR-Cas was clearly detrimental to pKJK5 (competitive ratio = -2.19 ± 0.11; $p < 0.001$).

In the naïve host, switching on CRISPR-Cas on its own benefitted pKJK5 (Figure 2E; competitive ratio 0.73 ± 0.1; $p = 0.0019$). When TA was switched on alongside this, there was no clear winner of the competition (competitive ratio = -0.21 ± 0.096; $p = 0.1$), however CRISPR-Cas still provided a benefit to pKJK5 relative to the scenario where CRISPR-Cas was switched off, where TA plasmid RP4 won the competition (competitive ratio = -0.94 ± 0.066; $p < 0.001$).

In addition, to determine whether our observed effects are driven by RP4's *parABCDE* TA system rather than other RP4-encoded mechanisms such as entry exclusion or incompatibility, we verified our conclusions by cloning the *par* operon onto a series of cloning vectors with different backbones of varying incompatibility group and offensively competing pKJK5 against these (Figure S2, Supplementary Results 2). This confirmed that CRISPR-Cas on its own benefits pKJK5, but if a competitor plasmid carries the *par* TA system, CRISPR-Cas is detrimental to pKJK5 in offense – regardless of competitor plasmid backbone.

Together, our experiments show that a defensive CRISPR-Cas system was always beneficial to its host plasmid — regardless of competitor TA status — in agreement with our core modelling predictions. These results were upheld during a mixed mode of CRISPR-Cas action, where CRISPR-Cas was never detrimental. In contrast, we found that the benefit of an offensive CRISPR-Cas system to its host plasmid depended on payload genes encoded on competitor plasmids; namely, a TA system on a competitor means that offensive CRISPR-Cas was detrimental to its plasmid.

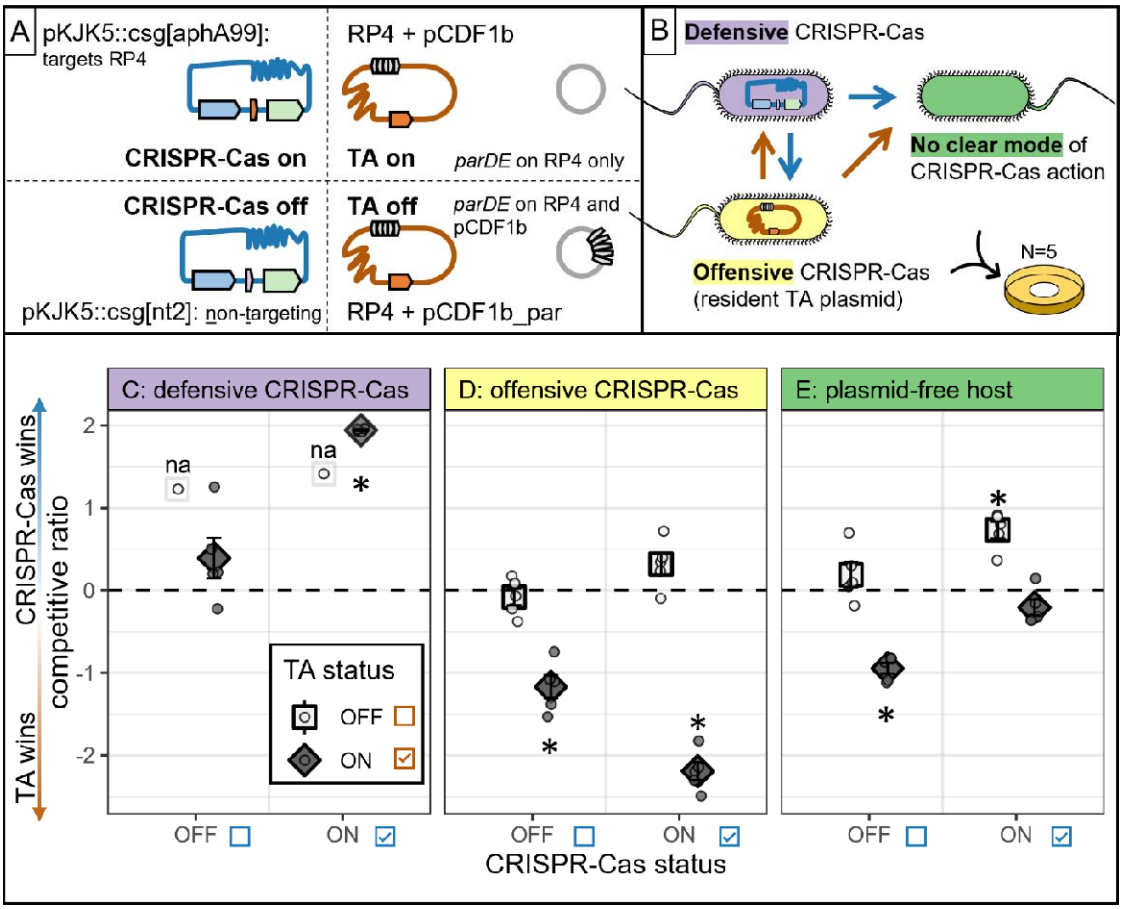

Figure 2: CRISPR-Cas is beneficial in defence but limited by TA in offense in experimental plasmid competition.

A: CRISPR-Cas and TA activity were tweaked on competitor plasmids in a binary manner by switching each system on or off. pKJK5::csg carries a gene cassette encompassing *cas9, sgRNA, GFP* with either an RP4-targeting or non-targeting guide, RP4 naturally carries TA system *parABCDE*. B: Plasmids were competed using three *E. coli* DH5α hosts with different plasmid content, allowing us to assess competitive outcome under defensive, offensive, or no clear mode of CRISPR-Cas action. After filter mating, plasmid content of each host was assessed by selective plating.

C-E: Mean ± standard error of the competitive ratio (log odds ratio of pKJK5-carrying hosts / RP4-carrying hosts) describes outcome of plasmid competition (N=5). Values >0 indicate CRISPR-Cas plasmid pKJK5 winning the competition, and values <0 indicate TA plasmid RP4 winning the competition for a certain host. The dashed line indicates a neutral outcome with competitive ratio = 0. Data are presented for treatments in which CRISPR-Cas and TA activity were toggled on or off in all combinations. Opacity of datapoints indicate number of replicates used to calculate means, this affects panel C TA-off data (N=1) and panel C TA-on & CRISPR-Cas-on data (N=4).

Stars indicate significant differences from 0 as assessed by T test and Bonferroni adjustment for multiple testing; *$p < 0.005$ with $\alpha = 0.005$; see Table 2 for all p values. na – not assessed due to N=1 after removal of missing values (no carriage of TA plasmid RP4 recorded in 4 out of 5 replicates).

<u>Plasmid-borne CRISPR-Cas systems preferentially target plasmids lacking TA systems.</u>

Our model and experiments suggest that the offensive benefits of plasmid-borne CRISPR-Cas systems are limited to conflicts where the competitor plasmid does not encode a TA system. To test whether this constraint is reflected in natural systems, we analysed genomic data to assess the association between CRISPR-Cas targeting and TA presence. If the fitness benefit of CRISPR-Cas systems in plasmid competition is limited by TA systems, we hypothesised that naturally occurring

plasmid-borne CRISPR-Cas systems would preferentially target plasmids without TA systems.

To answer this question, we analysed existing data on the plasmid-targeting spacers of plasmid-borne CRISPR-Cas systems [6], focusing on identifying which of these targeted plasmids encoded TA systems. The resulting targeting network provided a comprehensive picture of plasmids that were targeted by plasmid-borne CRISPR-Cas systems (N=1340), and the TA systems these targeted plasmids encoded (Figure 3A). Type II TA, including *parDE* (N=565), were most commonly identified. Within this network, 34% of plasmid-borne CRISPR-Cas systems were Type IV systems (Figure S4A), which function by repressing target gene expression, rather than causing nucleolytic cleavage [8,28]. This mode of action may allow targeted plasmids to persist without triggering PSK, potentially obscuring the relationship between targeting and TA presence. Indeed, Type IV-A1 and IV-A3-targeted plasmids have been shown to persist when targeted in non-essential regions [8,29]. Therefore, we repeated the analysis by partitioning the dataset into Type IV and non-Type IV systems. Restricting the data to non-Type IV systems reduced the number of targeted plasmids to 463, of which only 11% (N=51) encoded TA systems, and none encoded *parDE* (Figure S4B).

Correlational analyses on the partitioned data (all CRISPR-Cas types, Type IV only, and non-Type IV) yielded contrasting results. In all cases, Pearson's χ^2 tests confirmed a significant relationship between CRISPR-Cas targeting and TA presence (χ^2 = 94.08, 334.48, and 171.83, respectively; $p < 2.2\text{x}10^{-16}$), with small effect sizes (φ = 0.073, 0.137, and 0.098, respectively). When considering all plasmid-borne CRISPR-Cas types or Type IV only, TA-encoding plasmids were targeted more often than expected under the null hypothesis of no relationship between CRISPR-Cas

targeting and TA carriage (residuals = 7.21 and 13.82; $p = 5.71 \times 10^{-13}$ and 1.04×10^{-43}, respectively; Figure 3B). This contradicts our hypothesis that plasmid-borne CRISPR-Cas systems should preferentially target plasmids lacking TA systems. In contrast, when we excluded Type IV CRISPR-Cas systems, the association between CRISPR-Cas targeting and TA carriage reversed: fewer TA-encoding plasmids were targeted than expected (residual = -10; $p = 1.49 \times 10^{-23}$), consistent with our experimental data and model predictions.

Having established that non-Type IV plasmid-borne CRISPR-Cas systems preferentially target plasmids lacking TA systems, we next considered the few cases where they do target TA-encoding plasmids. Based on the expectation that such encounters would trigger PSK, we hypothesised that non-Type IV CRISPR-Cas plasmids would be more likely than Type IV CRISPR-Cas plasmids to encode compatible antitoxin families when targeting TA-encoding plasmids. To test this, we compared the frequency of compatible antitoxin families carried by plasmids with non-Type IV versus Type IV CRISPR-Cas systems when targeting TA+ plasmids. Compatible antitoxin families were present in 22% (15/69) of cases of non-Type IV targeting, but only 6% (352/5914) of Type IV cases (Figure 3C). Fisher's exact test confirmed enrichment in nucleolytic systems (OR = 4.4, 95% CI = 2.3–8, $p = 1.3 \times 10^{-5}$). A complementary binomial test, using the Type IV frequency (6%) as the empirical null, also showed significant enrichment of compatible antitoxin families in cases of non-Type IV targeting (observed = 22%, 95% CI = 13–33%, $p = 1.1 \times 10^{-5}$).

Overall, these results indicate that nucleolytic plasmid-borne CRISPR-Cas systems preferentially target plasmids lacking TA systems. This was observed with a modest effect size, which may be due to an additional propensity of plasmids with nucleolytic CRISPR-Cas systems to carry their own TA systems of the same family as found on

target plasmids, hypothetically ameliorating TA activity. These findings support our model and extend our experimental findings to natural systems across diverse CRISPR-Cas and TA system types. We conclude that nucleolytic, plasmid-borne CRISPR-Cas systems provide significant defensive benefits, even in the face of TA. In contrast, their benefits in offence are constrained by the presence of TA systems on competitor plasmids.

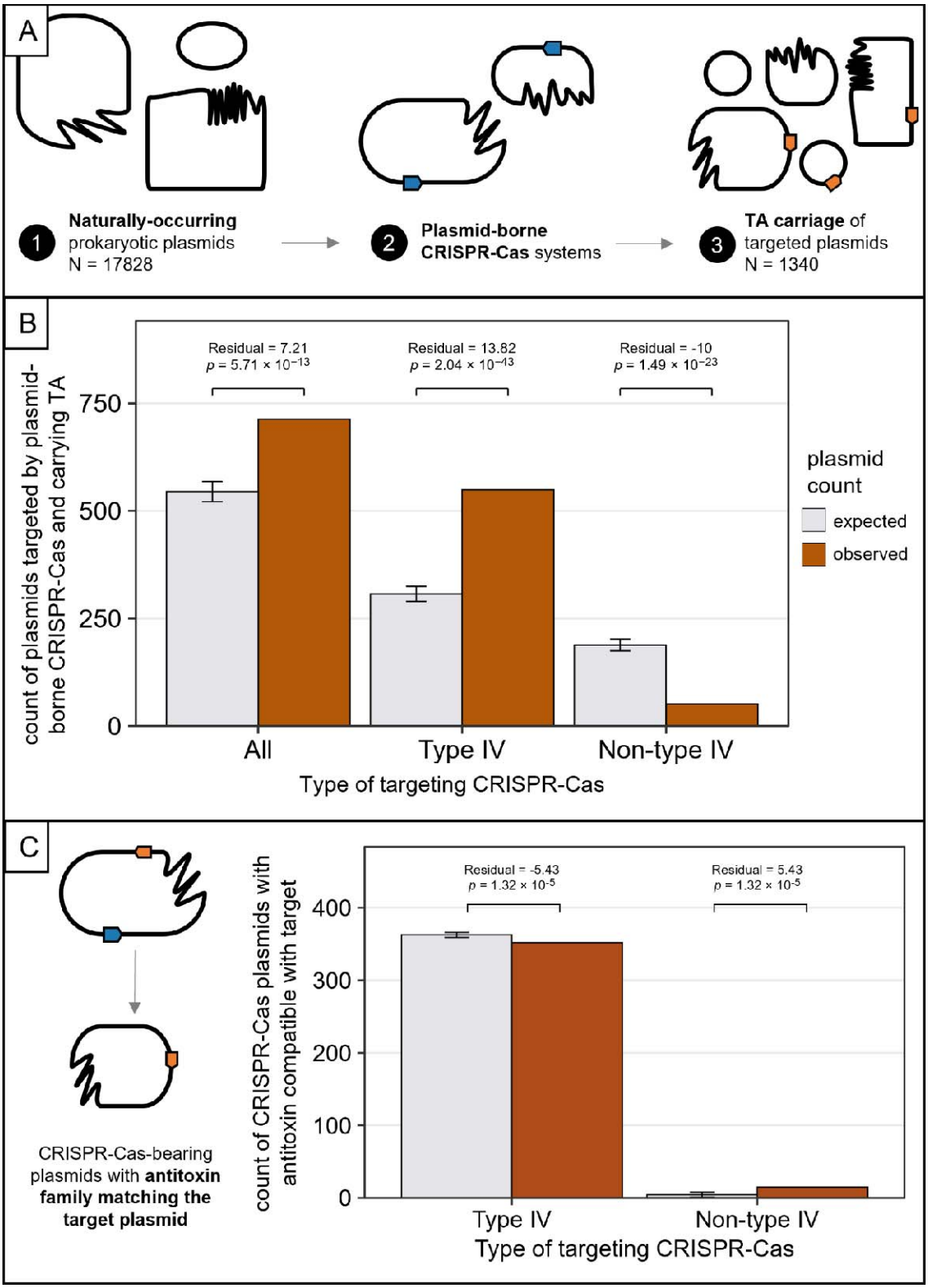

Figure 3: Plasmid-borne CRISPR-Cas systems (excluding Type IV) avoid targeting plasmids with toxin-antitoxin systems.

A: Naturally-occurring plasmid-borne CRISPR-Cas systems and the plasmids they target [6] were analysed for toxin-antitoxin (TA) carriage.

B: Comparison of observed vs. expected counts of targeted plasmids encoding TA by CRISPR-Cas type. Brown bars show the observed counts of plasmids in each group compared to the expected counts (grey bars) under the null hypothesis of independence between targeting and TA presence. Error bars represent standard error. Residuals and *p* values are presented after a Pearson's χ^2 test. Full contingency tables for all categories of plasmids can be found in Figure S5 (targeted or not targeted by CRISPR-Cas, coding or not coding for TA).

C: Comparison of observed vs. expected counts of CRISPR-Cas bearing plasmids carrying antitoxins of the same family as the target plasmid's TA system. Brown bars show the observed counts of plasmids in each group compared to the expected counts (grey bars) under the null hypothesis of independence between CRISPR-Cas targeting and the presence of compatible antitoxin families on the CRISPR-Cas plasmid. Error bars represent the 95% interval of counts expected under the null hypothesis of independence, calculated from the hypergeometric distribution. Residuals and *p* values are presented after a Fisher's exact test.

Discussion

Here, we examined the limitations of CRISPR-Cas in plasmid competition. Mathematical modelling predicted that when plasmids compete within co-infected cells, CRISPR-Cas can provide a benefit to the plasmid it resides on. However, when the competitor plasmid encodes a strong toxin-antitoxin (TA) system, CRISPR-Cas is only beneficial when defensive and resident in a host. Our experimental model system showed the same outcome as these core modelling predictions: offensive CRISPR-Cas becomes a liability when targeting a resident TA plasmid, while defensive and co-invading CRISPR-Cas provides a benefit even when competing against a TA plasmid. Finally, we further tested our theory and generalised our experimental findings by bioinformatically showing that plasmid-borne nucleolytic CRISPR-Cas systems avoid targeting other plasmids carrying TA systems or tend to carry their own TA systems of compatible families. In line with our experimental data, recent single-cell observations showed that chromosomal CRISPR-Cas systems (i.e., lacking an offensive capability) protected a population from invasion by TA-carrying plasmid RP4, even when TA was expressed [16].

TA was previously shown to be crucial to plasmid establishment, spread, and maintenance [17–19]. Our data adds to this broad utility of TA throughout a plasmid's life cycle, as we found TA contributing to its plasmid competitiveness in nearly all experimental scenarios (Figure 2). Underlining this, our model predicted that, unlike CRISPR-Cas (the benefit of which diminished when competing TA was stronger), TA became more beneficial in the presence of a stronger CRISPR-Cas response on the competitor plasmid (Figure 1; Supplementary Results 1). Regardless, TA and CRISPR-Cas show striking similarity: they benefit their own plasmid more when acting defensively than offensively (Figures 1-2). It is well established that plasmids

are more fit when residing in a host cell than when conjugating into a new host [30]. Conjugation itself is costly (e.g., by SOS-response activation [31]), a novel plasmid is associated with a high transient fitness cost [32], and existing plasmid-host pairs can benefit from compensatory mutations to ameliorate fitness costs [33]. Here, we add to this body of evidence by showing that specific plasmid-encoded genes, namely CRISPR-Cas and TA, also provide a higher benefit to vertically transferred plasmids than to those that are horizontally transferred when facing plasmid competition.

Recent modelling showed that plasmid cost is a key determinant of TA plasmid establishment in a bacterial population carrying (chromosomally encoded) CRISPR-Cas systems [34]. In support of this, the cost of plasmid co-infection was identified as a hurdle to plasmid establishment [35]. We do not directly measure plasmid costs in our experimental system, but our model assumes the presence of both CRISPR-Cas and TA is costly due to post-segregational killing (PSK). Experimentally, we are likely overinflating TA strength compared to natural populations: DH5α, our experimental host, is a recA- *E. coli* strain. RecA is implicated in *parDE* TA function, where recA- strains typically see survival rates ~3 orders of magnitude lower than recA+ strains [26]. Nevertheless, our bioinformatic analysis confirms the generalisability of our experimental results by revealing a negative association between plasmid-borne CRISPR-Cas targeting and competitor plasmid TA carriage.

Our findings help explain the distribution and mobility of microbial immune systems, where certain systems are more commonly found on specific MGEs rather than the bacterial chromosome [36,37]. Due to their offensive capability, plasmid-borne CRISPR-Cas systems are under different selective pressures than chromosomally encoded CRISPR-Cas systems – and therefore it is unsurprising that certain types of CRISPR-Cas are preferentially found on plasmids [6]. In our bioinformatics analysis,

only nucleolytic (non-Type IV) plasmid borne CRISPR-Cas systems avoid targeting plasmids carrying TA systems. Based on this, we hypothesise that plasmid-borne CRISPR-Cas systems can adopt different evolutionary strategies in light of competitor TA: a plasmid-borne CRISPR-Cas system could avoid targeting TA plasmids or become associated with compatible TA systems to overcome limitations caused by TA in offense, as showcased in our data and bioinformatics analysis. An alternative evolutionary scenario could involve the loss of nucleolytic activities, as seen for plasmid-borne Type IV and Type V-M [38] CRISPR-Cas systems. These would not have limitations in offense and can target TA-carrying plasmids without paying the costs of PSK induction. In addition, Type IV CRISPR-Cas systems may overcome TA activity by co-opting their host's spacer acquisition machinery [8,39] — this may strengthen Type IV CRISPR-Cas's role in defence (while resident in its host, the CRISPR-Cas system can acquire new spacers to defend from MGEs), while dampening its role in offense (when moving to a new host, the CRISPR-Cas system cannot acquire new spacers until it is expressed and therefore cannot target a newly encountered plasmid already present in the new host). The proposed evolutionary history of Type IV CRISPR-Cas systems supports the hypothesis that plasmid-borne CRISPR-Cas systems adopt different evolutionary strategies to remain effective in light of TA: nucleolytic Type III CRISPR-Cas lost its HD nuclease domain and diverged towards gene silencing activity by association with helicase DinG over evolutionary timescales [40]. Overall, the association between TA and the effectiveness of CRISPR-Cas in plasmid competition helps explain the distribution and mobility of bacterial defence systems and the propensity of certain defences to associate with particular MGEs.

Throughout this work, we assayed plasmid competition outcome within individual plasmid hosts. Despite this limitation, our work could inform predictions of community-level plasmid persistence. On a population level, within-host plasmid competition may be particularly relevant to highly permissive plasmid hosts — bacteria in which the cost of plasmid maintenance is low and which can cause persistence of plasmids on a community level [41,42], or in hosts closely associated with certain plasmid lineages, such as clinically problematic bacterial strains of *E. coli* Sequence Type 131 and their IncF plasmids [43]. A resident CRISPR-Cas plasmid in such highly permissive plasmid hosts may prevent their colonisation by TA-encoding competitor plasmids and thus prevent TA plasmid dissemination throughout the microbial community. In addition to making predictions about plasmid prevalence, our work can inform the use of CRISPR-Cas delivery tools (engineered plasmids used to directly kill or resensitise bacteria to antibiotics through removal of antimicrobial resistance-encoding plasmids [24,44]). Our work indicates that CRISPR-Cas delivery tools will be more effective when delivered prophylactically, i.e. when CRISPR-Cas is allowed to act defensively rather than offensively. When they are required to act offensively, other factors such as target plasmid copy number and compatibility can inform optimal CRISPR-Cas delivery tool design [45].

Here, we described how the relevance of plasmid-borne CRISPR-Cas to plasmid competition depends on its mode of action: defensive CRISPR-Cas is universally beneficial, but the benefit of offensive CRISPR-Cas can be limited by TA carried on competitor plasmids. This work underlines the utility of TA systems to plasmid competition and explains their abundance, and may help predict which plasmids can become established in clinically relevant species and communities. Further, we help

explain the distribution of bacterial immune systems by uncovering under which conditions plasmid-borne CRISPR-Cas systems are selected for, which will also inform the use of CRISPR-Cas based technologies.

Methods

Mathematical model

Mathematical modelling was carried out using Wolfram Mathematica v14.1. Equations E5 and E7 (see Supplementary Results 1) were imported into R version 4.3.2. Output plots were generated using RStudio version 2023.09.1+494 with the following packages: dplyr, ggplot2, and ggnewscale.

Plasmids and strains

Plasmids and strains used in this study are summarised in Table 1. *Escherichia coli* DH5α strains DH5α::CmR, DH5α::GmR, and DH5α::SmR were constructed by electroporating DH5α with pBAM1-Gm, pBAM1-Sm, and pBAM1-Cm [46,47] respectively and selecting for resistant recombinants; resistance gene insertion was confirmed by PCR and by verifying their respective resistant phenotypes after transfer in the absence of antibiotics.

RP4-targeting pKJK5::csg[aphA99] ('CRISPR-Cas on' version of pKJK5) was constructed using λ-red mediated recombineering and pKJK5 as a template, as described in [24] with the exception that *cas9*, *sgRNA* (programmed to target *aphA* with specificity AAATGGGCGCGTGATAAGGT) and *gfp* were inserted into pKJK5's *intI1* gene. Non-targeting control pKJK5::csg[nt2] ('CRISPR-Cas off' version of pKJK5) was previously published as pKJK5::gfp^{PL} [48] and carries a random non-functional *sgRNA*.

Vector pOGG99_par was constructed by deleting genes from pOPS0378 [49] to generate a minimal vector: *mCherry* was removed by digestion with EcoRI,

extraction, and re-ligation of the 6043 bp band. Next, site-directed mutagenesis of *aphA* was carried out using primers pOGG0_mut_fw and pOGG0_mut_rv and Thermo Scientific's site-directed mutagenesis kit according to manufacturer's instructions. In this way, the nucleotide at position 96 within *aphA* was silently mutated from C to G to bring the gene sequence in line with that found on our laboratory's version of RP4 and allow targeting by pKJK5::csg[aphA99]. Successful mutation was confirmed by Sanger sequencing of the finished plasmid using primer pOGG0_sequence. pOGG99 was constructed by excising *parABCDE* from pOGG99_par: pOGG99_par was digested with BlpI and BglII, the 3664 bp fragment was extracted and religated with annealed and phosphorylated linker oligos (pOGG99_parRemoval_top & btm). This yielded pOGG99, a version of pOGG99_par where *parABCDE* are replaced with a multiple cloning site module.

Vector pHERD99 was constructed by annealing oligos aphA99PAM_top and aphA99_btm and inserting them into pHERD30T's HindIII and KpnI restriction sites following standard molecular cloning protocols. Vector pSEVA251-99 was constructed by site-directed mutagenesis of pSEVA251's *aphA* gene as described for pOGG99_par above.

Vectors pCDF1b_par, pHERD99_par, and pSEVA251-99_par were constructed by *parABCDE* amplification using pOGG99_par as a template and primers par_fw and par_rv with high-fidelity Phusion polymerase (NEB) and insertion into pCDF1b, pHERD99's, and pSEVA251-99's KpnI restriction site respectively. This *parABCDE* operon is 99.96% identical to RP4's with a single nucleotide mismatch in the non-coding area between *parA* and *parB*.

All cloned plasmids were subjected to long-read sequencing by Plasmidsaurus using Oxford Nanopore Technology with custom analysis and annotation. Annotated sequences are deposited on Genbank with IDs listed in Table 1.

Table 1: Strains, Plasmids, and primers

Strains			
Name	**Shorthand**	**Notes**	**Reference**
Escherichia coli DH5α	DH5α		Common laboratory strain
Escherichia coli K12::mCherry	K12::mCherry	Chromosomal Km^R, mCherry, lacI insertion	[50]
Escherichia coli DH5α::CmR	DH5α::CmR	Chromosomal *cat* insertion	*This study*
Escherichia coli DH5α::GmR	DH5α::GmR	Chromosomal *aacC1* insertion	*This study*
Escherichia coli DH5α::SmR	DH5α::SmR	Chromosomal *aad* insertion	*This study*
Plasmids			
Plasmid	**Resistance and Payload**	**Notes**	**Reference**
pKJK5::csg [aphA99]	Tetracycline, Trimethoprim, CRISPR-Cas9 cassette targeted towards *aphA*	"CRISPR-Cas on" version of pKJK5::csg	*This study*
pKJK5::csg[nt2]	Tetracycline, Trimethoprim, non-targeting CRISPR-Cas9 cassette	"CRISPR-Cas off" version of pKJK5::csg. Previously referred to as pKJK5::gfp^{PL}	[48]
pHERD30T	Gentamicin	pBR322 vector	[51]
pHERD99	Gentamicin, includes [aphA99] target site	Genbank acc. OR900359	*This study*
pHERD99_par	Gentamicin, [aphA99] target site, *parABCDE*	Genbank acc. OR900360	*This study*
pCDF1b	Streptomycin		Novagen (EMD Millipore)

pCDF1b_par	Streptomycin, *parABCDE*	Genbank acc. OR900361	*This study*
pSEVA251	Kanamycin	IncQ vector; Genbank acc. JX560330	[52]
pSEVA251-99	Kanamycin (targetable by pKJK5::csg[aphA99])	Genbank acc. PV231316	*This study*
pSEVA251-99_par	Kanamycin, *parABCDE*	Genbank acc. PV231317	*This study*
pOPS0378	Kanamycin, mCherry, *parABCDE*	Addgene #133229	[49]
pOGG99	Kanamycin	IncP vector; Genbank acc. PV231318	*This study*
pOGG99_par	Kanamycin, *parABCDE*	Genbank acc. PV231319	*This study*
RP4	Tetracycline, Kanamycin, Ampicillin, *parABCDE*	Genbank acc. L27758	[53]
pBAM1-Gm	Ampicillin, Gentamicin	Tn5 *aacC1* transposon	[46]
pBAM1-Sm	Ampicillin, Streptomycin	Tn5 *aad* tranposon	[46]
pBAM1-Cm	Ampicillin, Chloramphenicol	Tn5 *cat* transposon	[47]
Primers and sequences			
Name	**Sequence (5' → 3')**		
[aphA99]	AAATGGGCGCGTGATAAGGT		
[nt2]	GTTTTCTGCCTGTCGATCCAGTTTTAGAGCTCTAAAACTGGATCGACAGGCAGAAAACATGTCGATCCA		
par_fw	TCGGTACCTGCATGAGCTTGTGGAAGTG		
par_rv	CAGGTACCTGCTCAACAGGTTCGCA		
aphA99PAM_top	AGCTTAAATGGGCGCGTGATAAGGTTGGTAC		
aphA99PAM_btm	CAACCTTATCACGCGCCCATTTA		
pOGG0_mut_fw	TGGGCGCGTGATAAGGTGGGTCAGAGCGGC		
pOGG0_mut_rv	TTTATAGCCATACAGATCCGCATCCATGTTGCTGTTCAGACGC		
pOGG0_sequence	TATTGGTGAGAATCCAGGCA		
pOGG99_parRemoval_top	TGAGCCAAGCTTGCATGCCTGCAGGTCGACTCTAGAGGATCCCCGGGTACCGAGCTCGAATTCACTA		
pOGG99_parRemoval_btm	GATCTAGTGAATTCGAGCTCGGTACCCGGGGATCCTCTAGAGTCGACCTGCAGGCATGCAAGCTTGGC		

Culture conditions

Unless otherwise stated, all strains were cultured shaking 180 rpm in LB broth or statically on LB plates at 37˚C. Where appropriate, cultures or plates were supplemented with the following antibiotics at the following concentrations: Ap – 100 µg/mL ampicillin; Cm – 25µg/mL chloramphenicol; Gm – 50 µg/mL gentamicin; Km – 50 µg/mL kanamycin; Sm – 50 µg/mL streptomycin; Tc – 12 µg/mL tetracycline; Tmp – 10 µg/mL trimethoprim.

Conjugation experiments

In three-strain competitions (Figure 2), bacterial hosts used were *E. coli* DH5α::SmR containing pKJK5::csg, *E. coli* DH5α::CmR containing RP4, and *E. coli* DH5α::GmR. All three strains either also contained empty vector pCDF1b, or pCDF1b_par for TA-off treatments. A control experiment (Figure S3) was set up in the same way, with the omission of bystander vectors pCDF1b or pCDF1b_par in all strains.

In two-strain competitions (Figure S2), *E. coli* DH5α::SmR containing pKJK5::csg was used as donor, and the recipient was *E. coli* DH5α::CmR containing either RP4, pHERD99, pSEVA251-99, pOGG99, or their *par*-encoding derivatives.

To turn CRISPR-Cas activity on or off, we used two different pKJK5::csg variants with fixed targeting specificity: pKJK5::csg[aphA99] was programmed to target RP4's *aphA* gene, and pKJK5::csg[nt2] encoded a non-functional sgRNA with a random 69-nt target sequence that is not present in the model system (plasmid pKJK5::gfp^{PL}; [48]).

Single colonies from streak plates of mating partners were suspended in 15-25 mL LB with antibiotics appropriate to maintain their plasmid content (see Table 1) and grown overnight. These T0 cultures were then washed twice with 0.9% (w/v) NaCl

and adjusted to OD600 = 0.5. Washed, OD-adjusted cultures were filter mated in a 1:1(:1) ratio:

Filter matings were carried out using a 12-stream Millipore vacuum pump, sterilised with 70% Ethanol and UV light before and after each batch of filter mating and assembled in a Cat2 biosafety cabinet. For each mating, a 0.22 µm glass microfibre filter (Whatman) was placed onto a vacuum pump position, dampened with 200 µL sterile 0.9% NaCl, and topped with a 0.22 µm cyclopore membrane (Whatman). Fully assembled filter positions were equilibrated by applying a vacuum until 2 mL of 0.9% NaCl were pumped through. Next, 1 mL of OD-adjusted donors and 1 mL of OD-adjusted recipients (or 600 µL of each mating partner in 3-strain competitions) were added to each filter position together with 1 mL 0.9% NaCl, and a vacuum applied until the strain mix was pumped through (N=5). Control matings always included donor-only, recipient-only (and naïve-strain-only where appropriate), and buffer-only sterility controls and yielded results as expected. Cyclopore membranes were placed cell-side-up onto a 10% LB plate (supplemented with 0.9% NaCl) and incubated at 37˚C for 36 hours. Then, cells were recovered by placing each filter into 3 mL of 0.9% NaCl and vortexed for 15 seconds. This cell suspension was frozen in 20% (w/v) glycerol at -70˚C and plated onto selective plates with various antibiotic regimes to assess strain prevalence and strains' plasmid content.

<u>Selective plating</u>

Samples were plated in 5 µL droplets in dilutions ranging from 10^{0}-10^{-7} onto LB medium containing different combinations of antibiotics. Cm, and Gm were used to select for DH5α::Cm and DH5α::Gm respectively, and combining these antibiotics with Tmp and Km allowed growth of only DH5α hosts carrying pKJK5 and RP4

respectively. Colonies were counted at the most appropriate dilution, and GFP fluorescence of pKJK5::csg-containing colonies confirmed stringency of selective regimes.

To assess overall sample composition and plasmid content of the DH5α::SmR host, we plated 50 µL of a 10^{-5} dilution of each replicate onto LB plates without selection and suspended 96 colonies of each sample in 250 µL LB each following overnight incubation. Previous assessment of colonies from selective plates sub-cultured on non-selective media indicated that RP4 and pKJK5::csg did not become lost over this timeframe in the absence of selection. The 96 clones picked from each replicate were then replica-stamped onto plates containing no selection, Cm, Gm, Km, and/or, Tmp. Clones growing on LB, but not LB supplemented with Cm or with Gm were scored as DH5α::SmR clones, and the Km / Tmp selective plates were used to score their plasmid content. Resistance to Km is conferred by *aphA*, which is the target of the CRISPR spacer on pKJK5::csg. In a control experiment, we nonetheless found selection using Km to be robust to assess RP4 presence (Figure S3).

<u>Plasmid competitive ratio</u>

We calculated pKJK5 and RP4's competitive ratio (log odds ratio) as follows:

$$competitive\ ratio = \log\left(\frac{\text{hosts containing pKJK5}}{\text{hosts containing RP4}}\right)$$

This gives a measure of which plasmid is more frequent in a certain host and therefore won the competition for the host at the end of the experiment. Positive competitive ratios indicate pKJK5 winning the competition, negative ratios indicate RP4 winning, and ratios ≈ 0 indicate equal carriage of pKJK5 and RP4 in the host.

<u>Statistical analyses</u>

Colony counts on all selective plates from all experiments, together with plasmid competitive ratios used to produce figures are available in supplementary material.

Data processing, data visualisation, and statistical analyses were carried out using R version 4.3.2 and RStudio version 2023.09.1+494 with the following packages: flextable, dplyr, readr, tidyr, ggplot2.

Competitive ratio

We carried out one-sample T tests and Bonferroni adjustment for multiple testing to test for significant differences of plasmid competitive ratio to 0, indicating either RP4 or pKJK5 winning the plasmid competition. Statistical significance of 'TA off' competitive ratio in DH5α::SmR could not be assessed due to N=1, as no RP4 carriage was recorded in most replicates. For all *p* values, see Table 2.

Table 2: T tests adjusted for multiple testing (Figure 2). Significant values after Bonferroni adjustment in bold. Host refers to *E. coli* DH5α chromosomal tag identity; S – SmR (defensive CRISPR-Cas), C – CmR (offensive CRISPR-Cas), G – GmR (naïve host).

CRISPR-Cas status	host	TA status	p value (unadjusted)
on	C	on	**0.0000366**
on	C	off	0.0720
on	G	on	0.0967
on	G	off	**0.00186**
on	S	on	**0.000000261**
off	C	on	**0.000998**
off	C	off	0.469
off	G	on	**0.000137**
off	G	off	0.266

CRISPR-Cas status	host	TA status	p value (unadjusted)
off	S	on	0.185

Bonferroni-adjusted significance threshold α = 0.005

Two-strain competitions with vectors showed different baseline competitive ratios dependent on vector identity. Therefore, we analysed relative differences in competitive ratio between treatments by fitting separate Generalised Linear Models to data generated in two-strain competitions (Figure S2).The inclusion of additional variables (e.g. replicate and position on filter pump) was tested, and the final models chosen for not including non-significant explanatory variables and upholding model assumptions. For model structures and coefficients see Table 3. RP4 (with bystander), pOGG99, pHERD99, and pSEVA251-99 data were followed up by Tukey's HSD test, see Table 4.

Table 3: GLM structures and coefficients for Figure S2.

RP4 with bystander model	comprat ~ CRISPR_status*TA_status				
	Estimate	Standard Error	z value	Pr(>|z|)	
(Intercept)	-0.178	0.822	-0.217	0.8306	
CRISPR_statusON	1.624	1.162	1.398	0.1792	
TA_statusON	0.010	1.162	0.009	0.9932	
CRISPR_statusON:TA_statusON	-5.345	1.743	-3.066	0.0067	**

*Signif. codes: 0 <= '***' < 0.001 < '**' < 0.01 < '*' < 0.05*

(Dispersion parameter for gaussian family taken to be 4.052162)
Null deviance: 142.7 on 21 degrees of freedom
Residual deviance: 72.94 on 18 degrees of freedom
(2 observations deleted due to missingness)

RP4 model	comprat ~ CRISPR_status				
	Estimate	Standard Error	z value	Pr(>|z|)	
(Intercept)	-0.150	0.062	-2.409	0.0737	.

CRISPR_statuson	-2.695	0.088	-30.687	0.0000	***

*Signif. codes: 0 <= '***' < 0.001 < '**' < 0.01 < '*' < 0.05*

(Dispersion parameter for gaussian family taken to be 0.0115664)
Null deviance: 10.94 on 5 degrees of freedom
Residual deviance: 0.04627 on 4 degrees of freedom

pOGG99 model comprat ~ CRISPR_status*TA_status

	Estimate	Standard Error	z value	Pr(>|z|)	
(Intercept)	-2.180	0.190	-11.486	0.0000	***
CRISPR_statusON	2.762	0.268	10.289	0.0000	***
TA_statusON	0.008	0.268	0.030	0.9765	
CRISPR_statusON:TA_statusON	-3.633	0.380	-9.570	0.0000	***

*Signif. codes: 0 <= '***' < 0.001 < '**' < 0.01 < '*' < 0.05*

(Dispersion parameter for gaussian family taken to be 0.108098)
Null deviance: 23.26 on 11 degrees of freedom
Residual deviance: 0.8648 on 8 degrees of freedom

pHERD99 model comprat ~ CRISPR_status*TA_status

	Estimate	Standard Error	z value	Pr(>|z|)	
(Intercept)	0.488	0.134	3.649	0.0065	**
CRISPR_statusON	3.360	0.189	17.769	0.0000	***
TA_statusON	-0.753	0.189	-3.982	0.0041	**
CRISPR_statusON:TA_statusON	-3.200	0.267	-11.970	0.0000	***

*Signif. codes: 0 <= '***' < 0.001 < '**' < 0.01 < '*' < 0.05*

(Dispersion parameter for gaussian family taken to be 0.05362118)
Null deviance: 34.01 on 11 degrees of freedom
Residual deviance: 0.429 on 8 degrees of freedom

pSEVA251-99 model comprat ~ CRISPR_status*TA_status

	Estimate	Standard Error	z value	Pr(>|z|)	
(Intercept)	0.056	0.127	0.440	0.6717	
CRISPR_statusON	0.218	0.180	1.211	0.2603	
TA_statusON	-0.234	0.180	-1.297	0.2308	
CRISPR_statusON:TA_statusON	-2.475	0.255	-9.710	0.0000	***

*Signif. codes: 0 <= '***' < 0.001 < '**' < 0.01 < '*' < 0.05*

(Dispersion parameter for gaussian family taken to be 0.04870928)
Null deviance: 14.59 on 11 degrees of freedom
Residual deviance: 0.3897 on 8 degrees of freedom

Table 4: Tukey's HSD results for Figure S2ACDE.

RP4 with bystander (CRISPR:TA status)	diff	lwr	upr	p value (adjusted)

off:off-on:on	3.71044989	0.03801164	7.382888	**4.7E-02**
off:on-on:on	3.72050983	0.04807158	7.392948	**4.6E-02**
on:off-on:on	5.33466862	1.66223037	9.007107	**3.4E-03**
off:on-off:off	0.01005995	-3.27466868	3.294789	9.9E-01
on:off-off:off	1.62421873	-1.66050990	4.908947	5.1E-01
on:off-off:on	1.61415879	-1.67056984	4.898887	5.2E-01
pOGG99 (CRISPR:TA status)	diff	lwr	upr	p value (adjusted)
off:off-on:on	0.863006847	0.003335675	1.7226780	**4.9E-02**
off:on-on:on	0.871163151	0.011491979	1.7308343	**4.7E-02**
on:off-on:on	3.625170716	2.765499544	4.4848419	**4.1E-06**
off:on-off:off	0.008156304	-0.851514868	0.8678275	9.9E-01
on:off-off:off	2.762163869	1.902492697	3.6218350	**3.2E-05**
on:off-off:on	2.754007565	1.894336393	3.6136787	**3.3E-05**
pHERD99 (CRISPR:TA status)	diff	lwr	upr	p value (adjusted)
on:on-off:on	0.1590421	-0.44642645	0.7645107	8.3E-01
off:off-off:on	0.7528541	0.14738553	1.3583227	**1.7E-02**
on:off-off:on	4.1123653	3.50689671	4.7178339	**7.5E-08**
off:off-on:on	0.5938120	-0.01165662	1.1992806	5.5E-02
on:off-on:on	3.9533232	3.34785456	4.5587918	**1.1E-07**
on:off-off:off	3.3595112	2.75404258	3.9649798	**4.7E-07**
pSEVA251-99 (CRISPR:TA status)	diff	lwr	upr	p value (adjusted)
off:on-on:on	2.2563024	1.6792313	2.8333734	**7.3E-06**
off:off-on:on	2.4900116	1.9129406	3.0670827	**3.5E-06**
on:off-on:on	2.7082955	2.1312244	3.2853665	**1.8E-06**
off:off-off:on	0.2337093	-0.3433617	0.8107803	5.9E-01
on:off-off:on	0.4519931	-0.1250779	1.0290642	1.3E-01
on:off-off:off	0.2182838	-0.3587872	0.7953549	6.4E-01

Streptomycin resistant c.f.u.

The log10 of proportion of streptomycin resistant c.f.u. presented in Figure S1 followed a normal distribution and was assessed by one-sample T tests and Bonferroni adjustment for multiple testing for differences to 0 (log10 of 1; complete maintenance of bystander vector pCDF1b). No differences were statistically significant (Table 6).

Table 6: T tests adjusted for multiple testing (Figure S1). Significant values after Bonferroni adjustment in bold.

CRISPR status	TA status	p value (unadjusted)
off	off	0.543
off	on	0.801
on	off	0.0414
on	on	0.985

Bonferroni-adjusted significance threshold α = 0.0125

Bioinformatic Analysis of plasmid TA carriage

The sequences of 17828 de-replicated plasmid found across prokaryotic genomes [6] were retrieved from NCBI using rentrez [54]. CRISPR-Cas presence and targeting information were adopted from [6]. Plasmid open reading frames were predicted with prodigal v2.6.3 [55]. Toxin-antitoxin nucleotide or protein sequences were retrieved from TADB v3.0 [14]. To identify complete toxin-antitoxin systems, plasmids were searched with BLAST v2.16.0 [56] and hits were filtered for cases where both a toxin and antitoxin component were directly adjacent. For the analysis of TA systems carried by CRISPR-Cas bearing plasmids, full TA systems were considered alongside orphan antitoxin genes, and a >70% alignment coverage in comparison with TADB was considered as a match. Counts of CRISPR loci, Cas loci, TA systems, and the network of TA families on plasmids carrying or targeted by CRISPR-Cas systems are available in supplementary material. Statistical analyses were run using R v4.4.2 base functions.

Acknowledgements

The authors would like to thank Mario Mestre (KU Copenhagen, Denmark) and Edze Westra (University of Exeter, UK) for stimulating and inspiring discussions and

enthusiasm. The authors further thank Iolanda Domingues (Exeter Centre for Cytomics, University of Exeter, UK) for valuable input with flow cytometry.

For the purpose of open access, the author has applied a 'Creative Commons Attribution (CC BY) licence to any Author Accepted Manuscript version arising from this submission.

Funding

DS was supported in part by grant MR/N0137941/1 for the GW4 BIOMED MRC DTP, awarded to the Universities of Bath, Bristol, Cardiff and Exeter from the Medical Research Council (MRC)/UKRI. JRR was supported by a summer studentship from the Lister Institute for Preventative Medicine. LJP and RPR were supported by research grant VIL60763 from VILLUM FONDEN. SPB acknowledges funding from the US National Science Foundation (NSF 2321502). WHG and SvH acknowledge funding from the JPI-AMR HARISSA programme (MISTAR; MR/W031191/1), and in addition SvH acknowledges funding from the Biotechnology and Biological Sciences Research Council (BB/R010781/1; BB/S017674/1) and the Lister Institute for Preventative Medicine.

The funders had no role in study design, data collection and analysis, decision to publish, or preparation of the manuscript.

DS, JRR, and LJP received a salary from JPI-AMR HARISSA, the Lister Institute for Preventative Medicine, and VILLUM FONDEN respectively.

References

1. Nazarian P, Tran F, Boedicker JQ. Modeling Multispecies Gene Flow Dynamics Reveals the Unique Roles of Different Horizontal Gene Transfer Mechanisms. 2018;9: 2978. doi:10.3389/fmicb.2018.02978

2. San Millan A, Heilbron K, MacLean RC. Positive epistasis between co-infecting plasmids promotes plasmid survival in bacterial populations. ISME J. 2014;8: 601–612. doi:10.1038/ismej.2013.182

3. Rocha EPC, Bikard D. Microbial defenses against mobile genetic elements and viruses: Who defends whom from what? PLOS Biol. 2022;20: e3001514. doi:10.1371/journal.pbio.3001514

4. Beamud B, Benz F, Bikard D. Going viral: The role of mobile genetic elements in bacterial immunity. Cell Host Microbe. 2024;32: 804–819. doi:10.1016/j.chom.2024.05.017

5. Makarova KS, Wolf YI, Iranzo J, Shmakov SA, Alkhnbashi OS, Brouns SJJ, et al. Evolutionary classification of CRISPR–Cas systems: a burst of class 2 and derived variants. Nat Rev Microbiol. 2020;18: 67–83. doi:10.1038/s41579-019-0299-x

6. Pinilla-Redondo R, Russel J, Mayo-Muñoz D, Shah SA, Garrett RA, Nesme J, et al. CRISPR-Cas systems are widespread accessory elements across bacterial and archaeal plasmids. Nucleic Acids Res. 2022;50: 4315–4328. doi:10.1093/nar/gkab859

7. Koonin EV, Makarova KS. CRISPR in mobile genetic elements: counter-defense, inter-element competition and RNA-guided transposition. BMC Biol. 2024;22: 295. doi:10.1186/s12915-024-02090-x

8. Benz F, Camara-Wilpert S, Russel J, Wandera KG, Čepaitė R, Ares-Arroyo M, et al. Type IV-A3 CRISPR-Cas systems drive inter-plasmid conflicts by acquiring spacers in trans. Cell Host Microbe. 2024;32: 875-886.e9. doi:10.1016/j.chom.2024.04.016

9. Mahendra C, Christie KA, Osuna BA, Pinilla-Redondo R, Kleinstiver BP, Bondy-Denomy J. Broad-spectrum anti-CRISPR proteins facilitate horizontal gene transfer. Nat Microbiol. 2020;5: 620–629. doi:10.1038/s41564-020-0692-2

10. Novick RP. Plasmid incompatibility. Microbiol Rev. 1987;51: 381–395. doi:10.1128/mr.51.4.381-395.1987

11. Roy D, Huguet KT, Grenier F, Burrus V. IncC conjugative plasmids and SXT/R391 elements repair double-strand breaks caused by CRISPR–Cas during conjugation. Nucleic Acids Res. 2020;48: 8815–8827. doi:10.1093/nar/gkaa518

12. Garcillán-Barcia MP, de la Cruz F. Why is entry exclusion an essential feature of conjugative plasmids? Plasmid. 2008;60: 1–18. doi:10.1016/j.plasmid.2008.03.002

13. Harms A, Brodersen DE, Mitarai N, Gerdes K. Toxins, Targets, and Triggers: An Overview of Toxin-Antitoxin Biology. Mol Cell. 2018;70: 768–784. doi:10.1016/j.molcel.2018.01.003

14. Guan J, Chen Y, Goh Y-X, Wang M, Tai C, Deng Z, et al. TADB 3.0: an updated database of bacterial toxin–antitoxin loci and associated mobile genetic elements. Nucleic Acids Res. 2024;52: D784–D790. doi:10.1093/nar/gkad962

700 15. Van Sluijs L, Van Houte S, Van Der Oost J, Brouns SJ, Buckling A, Westra ER. Addiction systems
701 antagonize bacterial adaptive immunity. FEMS Microbiol Lett. 2019;366: 47.
702 doi:10.1093/femsle/fnz047

703 16. Richards L, Lee D, Wiktor J, Cederblad J, Jones D. Molecular kinetics dictate population
704 dynamics in CRISPR-based plasmid defense. bioRxiv; 2025. p. 2025.03.27.645723.
705 doi:10.1101/2025.03.27.645723

706 17. Cooper TF, Heinemann JA. Postsegregational killing does not increase plasmid stability but acts
707 to mediate the exclusion of competing plasmids. Proc Natl Acad Sci. 2000;97: 12643–12648.
708 doi:10.1073/pnas.220077897

709 18. Cooper TF, Paixão T, Heinemann JA. Within-host competition selects for plasmid-encoded
710 toxin–antitoxin systems. Proc R Soc B Biol Sci. 2010;277: 3149–3155.
711 doi:10.1098/rspb.2010.0831

712 19. Rankin DJ, Turner LA, Heinemann JA, Brown SP. The coevolution of toxin and antitoxin genes
713 drives the dynamics of bacterial addiction complexes and intragenomic conflict. Proc R Soc B
714 Biol Sci. 2012;279: 3706–3715. doi:10.1098/rspb.2012.0942

715 20. Reuter A, Hilpert C, Dedieu-Berne A, Lematre S, Gueguen E, Launay G, et al. Targeted-
716 antibacterial-plasmids (TAPs) combining conjugation and CRISPR/Cas systems achieve strain-
717 specific antibacterial activity. Nucleic Acids Res. 2021;49: 3584–3598. doi:10.1093/nar/gkab126

718 21. Hale L, Lazos O, Haines AS, Thomas CM. An efficient stress-free strategy to displace stable
719 bacterial plasmids. Biotechniques. 2010;48: 223–228. doi:10.2144/000113366

720 22. Fraikin N, Couturier A, Lesterlin C. The winding journey of conjugative plasmids toward a novel
721 host cell. Curr Opin Microbiol. 2024;78: 102449. doi:10.1016/j.mib.2024.102449

722 23. Bahl MI, Hansen LH, Goesmann A, Sørensen SJ. The multiple antibiotic resistance IncP-1
723 plasmid pKJK5 isolated from a soil environment is phylogenetically divergent from members of
724 the previously established α, β and δ sub-groups. Plasmid. 2007;58: 31–43.
725 doi:10.1016/j.plasmid.2006.11.007

726 24. Sünderhauf D, Klümper U, Pursey E, Westra ER, Gaze WH, van Houte S. Removal of AMR
727 plasmids using a mobile, broad host-range CRISPR-Cas9 delivery tool. Microbiology. 2023;169:
728 001334. doi:10.1099/mic.0.001334

729 25. Adamczyk M, Jagura-Burdzy G. Spread and survival of promiscuous IncP-1 plasmids. Acta
730 Biochim Pol. 2003;50: 425–453. doi:10.18388/abp.2003_3696

731 26. Fraikin N, Van Melderen L. Single-cell evidence for plasmid addiction mediated by toxin–
732 antitoxin systems. Nucleic Acids Res. 2024;52: 1847–1859. doi:10.1093/nar/gkae018

733 27. Roberts RC, Ström AR, Helinski DR. The parDE Operon of the Broad-host-range Plasmid RK2
734 Specifies Growth Inhibition Associated with Plasmid Loss. J Mol Biol. 1994;237: 35–51.
735 doi:10.1006/jmbi.1994.1207

736 28. Čepaitė R, Klein N, Mikšys A, Camara-Wilpert S, Ragožius V, Benz F, et al. Structural variation of
737 types IV-A1- and IV-A3-mediated CRISPR interference. Nat Commun. 2024;15: 9306.
738 doi:10.1038/s41467-024-53778-1

739 29. Sanchez-Londono M, Rust S, Hernández-Tamayo R, Gomes-Filho JV, Thanbichler M, Randau L.
740 Visualization of Type IV-A1 CRISPR-mediated repression of gene expression and plasmid
741 replication. Nucleic Acids Res. 2024;52: 12592–12603. doi:10.1093/nar/gkae879

742 30. San Millan A, MacLean RC. Fitness costs of plasmids: a limit to plasmid transmission. Microbiol
743 Spectr. 2017;5: 5.5.02. doi:10.1128/microbiolspec.MTBP-0016-2017

744 31. Baharoglu Z, Bikard D, Mazel D. Conjugative DNA Transfer Induces the Bacterial SOS Response
745 and Promotes Antibiotic Resistance Development through Integron Activation. PLOS Genet.
746 2010;6: e1001165. doi:10.1371/journal.pgen.1001165

747 32. Prensky H, Gomez-Simmonds A, Uhlemann A, Lopatkin AJ. Conjugation dynamics depend on
748 both the plasmid acquisition cost and the fitness cost. Mol Syst Biol. 2021;17.
749 doi:10.15252/msb.20209913

750 33. Hall JPJ, Wright RCT, Guymer D, Harrison E, Brockhurst MA. Extremely fast amelioration of
751 plasmid fitness costs by multiple functionally diverse pathways. Microbiology. 2019;166.
752 doi:10.1099/mic.0.000862

753 34. Siedentop B, Losa Mediavilla C, Kouyos RD, Bonhoeffer S, Chabas H. Assessing the Role of
754 Bacterial Innate and Adaptive Immunity as Barriers to Conjugative Plasmids. Mol Biol Evol.
755 2024;41: msae207. doi:10.1093/molbev/msae207

756 35. Igler C, Huisman JS, Siedentop B, Bonhoeffer S, Lehtinen S. Plasmid co-infection: linking
757 biological mechanisms to ecological and evolutionary dynamics. Philos Trans R Soc B Biol Sci.
758 2021;377: 20200478. doi:10.1098/rstb.2020.0478

759 36. Georjon H, Bernheim A. The highly diverse antiphage defence systems of bacteria. Nat Rev
760 Microbiol. 2023;21: 686–700. doi:10.1038/s41579-023-00934-x

761 37. Patel PH, Maxwell KL. Prophages provide a rich source of antiphage defense systems. Curr Opin
762 Microbiol. 2023;73: 102321. doi:10.1016/j.mib.2023.102321

763 38. Wu WY, Mohanraju P, Liao C, Adiego-Pérez B, Creutzburg SCA, Makarova KS, et al. The
764 miniature CRISPR-Cas12m effector binds DNA to block transcription. Mol Cell. 2022;82: 4487-
765 4502.e7. doi:10.1016/j.molcel.2022.11.003

766 39. Newire E, Aydin A, Juma S, Enne VI, Roberts AP. Identification of a Type IV-A CRISPR-Cas System
767 Located Exclusively on IncHI1B/IncFIB Plasmids in Enterobacteriaceae. Front Microbiol.
768 2020;11. doi:10.3389/fmicb.2020.01937

769 40. Moya-Beltrán A, Makarova KS, Acuña LG, Wolf YI, Covarrubias PC, Shmakov SA, et al. Evolution
770 of Type IV CRISPR-Cas Systems: Insights from CRISPR Loci in Integrative Conjugative Elements of
771 Acidithiobacillia. CRISPR J. 2021 [cited 2 Jan 2025]. doi:10.1089/crispr.2021.0051

772 41. Li L, Dechesne A, He Z, Madsen JS, Nesme J, Sorensen SJ, et al. Estimating the Transfer Range of
773 Plasmids Encoding Antimicrobial Resistance in a Wastewater Treatment Plant Microbial
774 Community. 2018; acs.estlett.8b00105. doi:10.1021/acs.estlett.8b00105

775 42. Alonso-del Valle A, León-Sampedro R, Rodríguez-Beltrán J, DelaFuente J, Hernández-García M,
776 Ruiz-Garbajosa P, et al. Variability of plasmid fitness effects contributes to plasmid persistence
777 in bacterial communities. Nat Commun. 2021;12: 2653. doi:10.1038/s41467-021-22849-y

43. Kondratyeva K, Salmon-Divon M, Navon-Venezia S. Meta-analysis of Pandemic Escherichia coli ST131 Plasmidome Proves Restricted Plasmid-clade Associations. Sci Rep. 2020;10: 36. doi:10.1038/s41598-019-56763-7

44. Pursey E, Sünderhauf D, Gaze WH, Westra ER, van Houte S. CRISPR-Cas antimicrobials: Challenges and future prospects. Hogan DA, editor. PLOS Pathog. 2018;14: e1006990. doi:10.1371/journal.ppat.1006990

45. Kippnich J, Benz F, Uecker H, Baumdicker F. Effectiveness of CRISPR-Cas in Sensitizing Bacterial Populations with Plasmid-Encoded Antimicrobial Resistance. bioRxiv; 2024. p. 2024.07.05.602127. doi:10.1101/2024.07.05.602127

46. Martínez-García E, Calles B, Arévalo-Rodríguez M, de Lorenzo V. pBAM1: an all-synthetic genetic tool for analysis and construction of complex bacterial phenotypes. BMC Microbiol. 2011;11: 38. doi:10.1186/1471-2180-11-38

47. Dimitriu T, Kurilovich E, Łapińska U, Severinov K, Pagliara S, Szczelkun MD, et al. Bacteriostatic antibiotics promote CRISPR-Cas adaptive immunity by enabling increased spacer acquisition. Cell Host Microbe. 2022;30: 31-40.e5. doi:10.1016/j.chom.2021.11.014

48. Sünderhauf D, Klümper U, Gaze WH, Westra ER, Van Houte S. Interspecific competition can drive plasmid loss from a focal species in a microbial community. ISME J. 2023 [cited 29 Aug 2023]. doi:10.1038/s41396-023-01487-w

49. Mendoza-Suárez MA, Geddes BA, Sánchez-Cañizares C, Ramírez-González RH, Kirchhelle C, Jorrin B, et al. Optimizing Rhizobium-legume symbioses by simultaneous measurement of rhizobial competitiveness and N2 fixation in nodules. Proc Natl Acad Sci. 2020;117: 9822–9831. doi:10.1073/pnas.1921225117

50. Klümper U, Riber L, Dechesne A, Sannazzarro A, Hansen LH, Sørensen SJ, et al. Broad host range plasmids can invade an unexpectedly diverse fraction of a soil bacterial community. ISME J. 2015;9: 934–945. doi:10.1038/ismej.2014.191

51. Qiu D, Damron FH, Mima T, Schweizer HP, Yu HD. PBAD-based shuttle vectors for functional analysis of toxic and highly regulated genes in Pseudomonas and Burkholderia spp. and other bacteria. Appl Environ Microbiol. 2008;74: 7422–7426. doi:10.1128/AEM.01369-08

52. Silva-Rocha R, Martínez-García E, Calles B, Chavarría M, Arce-Rodríguez A, de las Heras A, et al. The Standard European Vector Architecture (SEVA): a coherent platform for the analysis and deployment of complex prokaryotic phenotypes. Nucleic Acids Res. 2013;41: D666–D675. doi:10.1093/nar/gks1119

53. Pansegrau W, Lanka E, Barth PT, Figurski DH, Guiney DG, Haas D, et al. Complete Nucleotide Sequence of Birmingham IncPa Plasmids. J Mol Biol. 1994; 623–663.

54. Winter DJ. rentrez: An R package for the NCBI eUtils API. R J. 2017;9: 520–526.

55. Hyatt D, Chen G-L, LoCascio PF, Land ML, Larimer FW, Hauser LJ. Prodigal: prokaryotic gene recognition and translation initiation site identification. 2010;11: 119. doi:10.1186/1471-2105-11-119

56. Camacho C, Coulouris G, Avagyan V, Ma N, Papadopoulos J, Bealer K, et al. BLAST+: architecture and applications. BMC Bioinformatics. 2009;10: 421. doi:10.1186/1471-2105-10-421

List of Supporting Information Legends

Supplementary Results 1-3

Table S1: Default parameter values and rationales for graphical analyses.

Figure S1: Mean ± standard error of the proportion of Streptomycin resistant Colony Forming Units (CFU) after mating was never significantly different from 1 (T test followed by Bonferroni adjustment for multiple testing; Table 6).

Figure S2: Outcome of competition with cloning vectors. Mean ± standard error of the competitive ratio (log10 of pKJK5-carrying hosts / competitor-carrying hosts) describes the outcome of plasmid competition (N=5). Values <0 indicate CRISPR-Cas plasmid pKJK5 winning the competition, and values >0 indicate the TA competitor plasmid winning the competition for a DH5α host where CRISPR-Cas was acting offensively. Data are presented for treatments in which CRISPR-Cas and TA activity were toggled on or off in all combinations. RP4 competition outcome (A-B) in this simplified model system matched the outcome observed earlier (Figure 2B). Relative differences between treatments are indicated with grey lines and were assessed by Tukey's HSD after fitting individual Generalised Linear Models; see methods and Table 3-4 for model details and p values. *p<0.05; ***p<0.001; n.s. not significant p>0.63.

Figure S3: Assessed RP4 proportion is largely robust to antibiotic used to select for RP4.

Mean and standard error of RP4 content of hosts in pilot mating experiment lacking a bystander plasmid assessed by ampicillin or by kanamycin, N=5. Data are presented for CRISPR-Cas switched on or off.

Figure S4: Plasmid-borne CRISPR-Cas systems and their targets.

A: CRISPR-Cas systems encoded on plasmids; split into distribution of Cas operon and CRISPR array types. Type IV systems are highlighted to emphasize their predominance

B: The total number of plasmids encoding each TA family, highlighting *parDE* and other well-studied post-segregational killing (PSK) systems [13]. The other bar charts show the proportion of plasmids encoding each TA family targeted by plasmid borne Type IV and non-Type IV CRISPR-Cas systems.

Figure S5: Contingency tables of expected versus observed values for the association between plasmid-borne CRISPR-Cas targeting and TA carriage.

Contingency tables showing the relationship between plasmid targeting and TA presence. The tables display the observed counts of plasmids with or without TA systems and whether they are targeted or not by CRISPR spacers in another plasmid, either for all CRISPR-Cas types (A), Type IV CRISPR-Cas only (B), or for non-Type IV CRISPR-Cas (C). The bar plots show the sum of counts for each vertical or horizontal group. Facets in the table are coloured by standardised residual after Pearson's χ^2 test, indicating magnitude and directionality of association (red – less than expected, blue – more than expected).

Supplementary Data

Three-strain competition (Figure 2)

Raw data (direct)
Raw counts and dilution factor counted at ("-3" means colonies were counted at a 10^-3 dilution) for each sample.

Raw data (stamp)
Binary data indicating how many colonies grew in 96 well plate for each sample (LB), and on each selective plate. true – growth; false – no growth.

Proportional data and competitive ratio (Figure 2)
'readout' indicates which readout method was used to calculate plasmid proportion. 'Direct_selection' refers to direct selective plating; 'stamp_plating' refers to stamp plating. Columns "pKJK5" and "RP4" indicate the proportion of each host occupied by the respective plasmid, "competitive_ratio" is plotted in Figure 2.

StrepR plating
CFU/mL derived from triplicate droplet plates of each sample as above, on LB (total), Cp, Gm, and Sm selective plates. S_prop is the ratio of Sm / total and is plotted in Figure S1.
Note that these plate counts were derived from frozen glycerol stocks of the experiment above at a different time, so absolute CFU/mL do not exactly correspond with values in the first data tab.

Raw data (Figure S3)
Proportion of hosts carrying RP4 assessed by selective plating using Ampicillin or Kanamycin after a pilot experiment lacking bystander plasmids. Hosts include S (DH5a::SmR; pKJK5 host), C (DH5a::CmR; RP4 host), and G (DH5a::GmR; naïve host).

Two-strain competitions (Figure S2)

Raw data
"Batch" and "Position" refer to where in the vacuum pump the sample was included. These variables were included in test statistical models and found not to be significant / significant only because of their correlation with treatment.
Donor / Recipient OD pre- and post-adjust refer to measured OD600 of strains before and after washing and adjusting OD. These variables were included in test statistical models and found not to be significant / significant only because of their correlation with treatment.
"Selective Plate" and "Plate Type" refer to selective plate colonies were counted on. Plate type describes which colony identity was expected in clear text. C - Chloramphenicol, T - Trimethoprim, K - Kanamycin, G - Gentamicin.

Competitive Ratio
"Batch" and "Position" as above.
"comprat" is the competitive ratio and is plotted in Figure S2.

Bioinformatics dataset (Figure S4)

Cas counts
Plasmid-borne Cas operon types; Figure S4A

CRISPR counts
Plasmid-borne CRISPR array types; Figure S4A

TA counts
Counts of TA systems on plasmids targeted by plasmid-borne CRISPR-Cas systems; Figure S4B

TA compatibility network
TA families on targeted plasmids (Target), alongside antitoxin (AT) families on targeting CRISPR-Cas plasmids (Source)

Bioinformatics statistical analysis (Figure 3, Figure S5)

observed vs expected (3B)
data for and test statistics after chi-squared test presented in Figure 3B. Note that all data are presented in contingency tables in Figure S5, but only the data for has_ta = TRUE & targeted = TRUE are presented in Figure 3

observed vs expected (3C)
data for and test statistics after Fisher's exact test presented in Figure 3C.